Combination of photodynamic therapy and stimulator of interferon genes (STING) agonist inhibits colorectal tumor growth and recurrence

Hao, Y.; Ma, S.; Gu, Z.L.; Haghparast, A.; Schomann, T.; Yu, Z.F.; ... ; Dijke, P. ten

Received: 20 September 2022 | Revised: 12 November 2022 | Accepted: 27 December 2022

DOI: 10.1002/cac2.12405

CANCER COMMUNICATIONS Open Access

LETTER TO THE EDITOR

Combination of photodynamic therapy and stimulator of interferon genes (STING) agonist inhibits colorectal tumor growth and recurrence

Dear Editor,

Great progress has been made in the clinical use of photodynamic therapy (PDT) for the treatment of patients with superficial tumors [1]. However, cancer recurrence and metastasis have limited the application of PDT in the treatment of solid tumors and advanced cancers. In this context, combining PDT with other complementary immunotherapy regimens may overcome these limitations of PDT [2]. Therefore, we aimed to elucidate the inhibitory efficiency of PDT in combination with an agonist stimulator of interferon genes (STING) in colorectal cancer (CRC) models and to explore the underlying regulatory effects on the host immune system. STING agonists play an important role in the induction of innate anti-tumor immunity on tumor growth and recurrence potential. All methods used in this work are described in the Supplementary Material.

First, we showed that the photosensitizer verteporfin® was internalized into CRC MC38 and CT26 cells 3 h after incubation and effectively induced cell death by generating reactive oxygen species (ROS) after irradiation (Figure 1A-B and Supplementary Figure S1). PDT-induced dying tumor cells could be phagocytosed by dendritic cells (DCs) (Figure 1C), which in turn stimulated the phenotypic maturation of DCs [3]. Furthermore, ADU-S100 (synthetic cyclic dinucleotides that activate the cyclic GMP-AMP synthase [cGAS]-STING pathway) amplified this immunological effect of PDT-treated cells on DC activation, as shown by the increased expression of CD86 and major histocompatibility complex (MHC)-II (Figure 1D and Supplementary Figure S2). We explored the effect of PDT-treated cells and ADU-S100 on the polarization state of macrophages. Although PDT-treated cells did not alter the polarization state of bone marrow-derived macrophages (BMDMs) in vitro, treatment with ADU-S100 could re-polarize anti-inflammatory M2-type BMDMs [4] toward the pro-inflammatory M1 phenotype; shown by the increased mRNA expression of M1 markers, surface polarization protein level and production of inflammatory mediators, as well as the decreased expression of key M2 markers (Supplementary Figure S3).

The accumulation of photosensitizers at tumor sites is a prerequisite for PDT. We confirmed that verteporfin was efficiently accumulated in tumors but was also found in metabolic organs (Supplementary Figure S4). Importantly, since the near-infrared (NIR)-laser is a local treatment, no side effect is expected in other organs. Next, we investigated the anti-tumor effects of PDT in combination with ADU-S100 via immunocompetent syngeneic CRC mouse models (Figure 1E). The results showed that the combination of PDT with ADU-S100 exerted a highly suppressive effect on tumor growth and cell proliferation compared to the mild and moderate effects of PDT and ADU-S100 monotherapy, respectively (Figure 1F-G and Supplementary Figure S5A-C). Kaplan-Meier survival curve analysis revealed that the combination of PDT with ADU-S100 almost completely eradicated the MC38 tumors of tumor-bearing mice (survival probability, 91%) compared with PDT (survival probability, 22%) or ADU-S100 (survival probability, 64%) monotherapy (Figure 1H). The same trend was confirmed in the CT26 model (Supplementary Figure S5D-G).

PDT and ADU-S100 have been reported to exert anti-tumor effects by converting the tumor microenvironment (TME) and the tumor-draining lymph nodes (dLNs) from an immunosuppressive to a pro-inflammatory state [2, 5]. As shown in Figure 1I, 3 h after the first ADU-S100 treatment, tumors treated with combinational therapy showed a higher expression of genes encoding pro-inflammatory cytokines [9] than tumors subjected to monotherapies.

Abbreviations: BMDMs, bone marrow-derived macrophages; cGAS, cyclic GMP-AMP synthase; CRC, colorectal cancer; DCs, dendritic cells; H&E, hematoxylin and eosin; IFN, interferon; IgG, immunoglobulin G; IL, interleukin; MHC, major histocompatibility complex; NIR, near-Infrared; PDT, photodynamic therapy; ROS, reactive oxygen species; STING, stimulator of interferon genes; dLNs, tumor-draining lymph nodes; TME, tumor microenvironment; VP, Verteporfin.

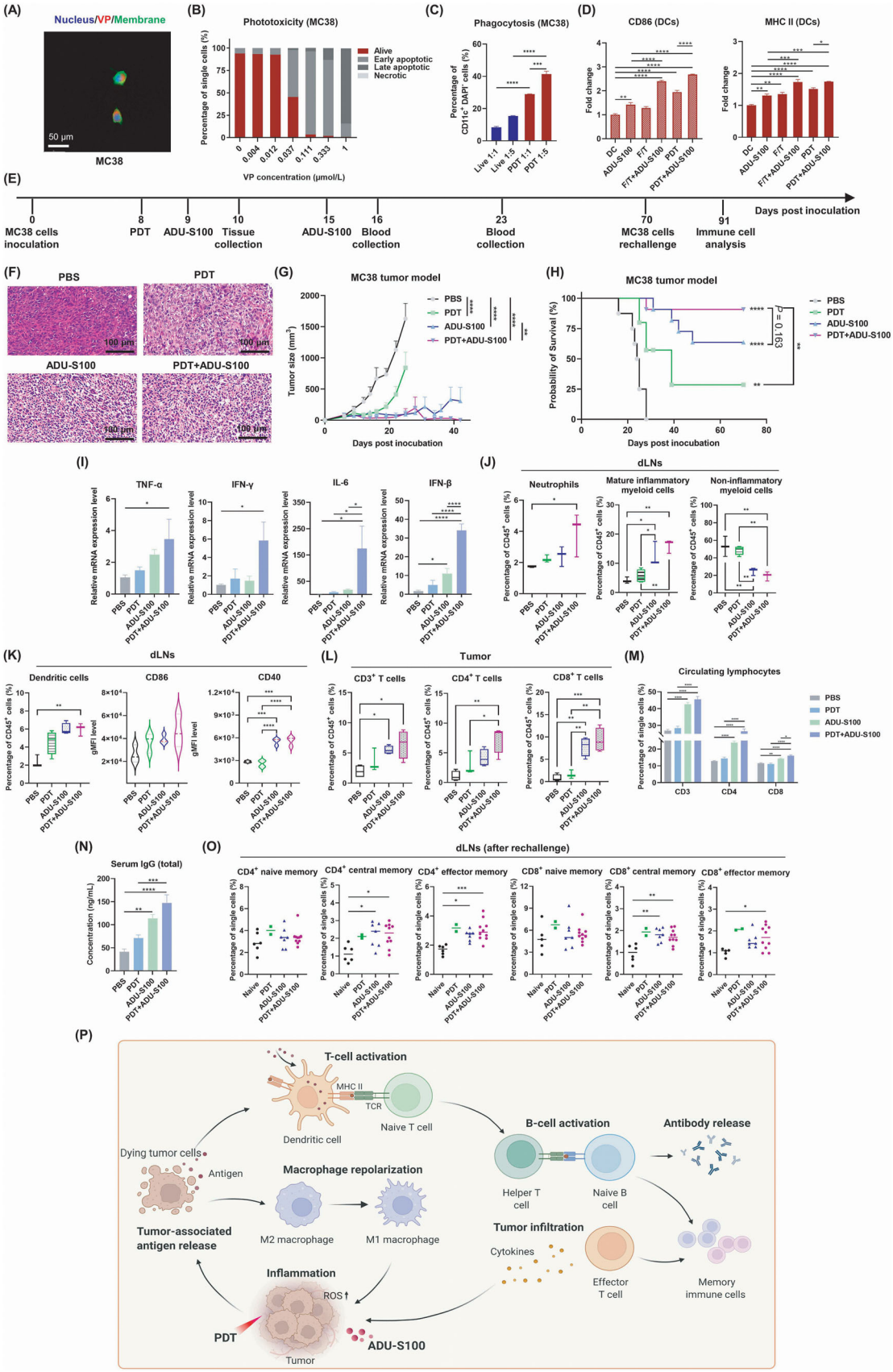

FIGURE 1 **Combination of Verteporfin-supported PDT with ADU-S100 cooperatively modulates the TME, thereby mediating anti-tumor immunity in CRC mice model**. (**A**) Typical fluorescence microscopy images of MC38 cells taken 3 h after incubation with 0.5 μmol/L VP. Scale bar = 50 μm.VP can be rapidly taken up into the MC38 tumor cells. (**B**) The phototoxic effects of VP in MC38 cells were investigated by flow cytometry analysis. Single cells were gated into live cells (FITC$^-$DAPI$^-$), early apoptotic cells (FITC$^+$DAPI$^-$), late apoptotic cells (FITC$^+$DAPI$^+$) and necrotic cells (FITC$^-$DAPI$^+$). VP by itself is not directly toxic to the MC38 tumor cells

in the absence of light irradiation; however, it can effectively cause cancer cell death after exposure to light from a 690 nm laser. (**C**) PDT-treated MC38 tumor cell debris phagocytosed by DCs after 2 h of co-culturing in two different ratios (1:1 and 1:5) immediately post-treatment. Phagocytosis of DCs was measured by determining the percentage of $CD11c^+CMFDA^+$-double positive populations as the mean values ± SEM. PDT-induced dying MC38 tumor cells could be phagocytosed by DCs. (**D**) The graphs show the mean gMFI ± SEM of CD86 (left panel) and MHC-II (right panel) on DCs after 24 h co-culture with ADU-S100, dying MC38 tumor cells induced by three freeze/thaw cycle treatments at -20°C (F/T), dying MC38 tumor cells induced by VP-PDT treatment or the combination of dying MC38 tumor cells and ADU-S100 by flow cytometric analysis. PDT-induced dying tumor cells could be phagocytosed by DCs. which in turn stimulated the phenotypic maturation of DCs, while ADU-S100 amplified this immunological effect of PDT-treated MC38 cells on DCs activation. (**E**) Schematic representation of the time course and administration regimen for MC38 tumor-bearing mice was shown. Tumor-bearing mice were treated with PDT, and the next day, two intra-tumoral injections of ADU-S100 were administered at one-week intervals. (**F**) Representative H&E staining images of MC38 tumors on day 10 after mice received different treatments. Scale bar = 100 μm. A large number of tumor cells with large nuclei and abundant vascular interstitium were visible in the control section. In contrast, in the treatment groups, the membranes of some tumor cells were disrupted and fused with intercellular material to form faint erythema; the damage extent was mildest in the PDT group, moderate in the ADU-S100 group, and highest in the COMB group. (**G**) Average tumor size of MC38 tumors over time, and data are expressed as mean ± SEM: Control vs. PDT $P < 0.0001$; Control vs. ADU-S100 $P < 0.0001$; Control vs. PDT + ADU-S100 $P < 0.0001$; PDT vs. PDT + ADU-S100 $P < 0.0001$; ADU-S100 vs. PDT + ADU-S100 $P = 0.0015$. The log-rank test was used to assess the statistical significance of survival time. Two-way ANOVAs were used for the statistical analysis of the significance of tumor volume and statistical differences were considered significant at * $P < 0.05$, ** $P < 0.01$, *** $P < 0.001$, **** $P < 0.0001$. Either PDT or ADU-S100 had an inhibitory effect on the progression of tumor growth, but the combinational therapy had the highest effect. (**H**) Percentage survival of MC38 tumor-bearing mice receiving different treatments: Control vs. PDT p = 0.0019; Control vs. ADU-S100 $P < 0.0001$; Control vs. PDT + ADU-S100 $P < 0.0001$; PDT vs. PDT + ADU-S100 $P = 0.0065$; ADU-S100 vs. PDT + ADU-S100 $P = 0.1627$. The log-rank test was used to assess the statistical significance of survival time and statistical differences were considered significant at * $P < 0.05$, ** $P < 0.01$, *** $P < 0.001$, **** $P < 0.0001$. The combinational therapy significantly improved the survival time of MC38 tumor-bearing mice compared to single therapies. (**I**) Inflammation-associated gene expression by qRT-PCR in tumors 3 h after the first ADU-S100 treatment for all groups. Three hours after the first ADU-S100 treatment, tumors treated with combinational therapy showed higher expression of genes encoding pro-inflammatory cytokines: TNF-α, IFN-γ, IL-6, and IFN-β compared to tumors subjected to single treatments. (**J**) Flow cytometry analysis of inflammation-associated cell populations in dLNs on day 10 from mice received different treatments. Living ($DAPI^-$) $CD45^+$ cells were further gated to neutrophils ($CD11b^+Ly6G^+$), mature inflammatory myeloid cells ($CD11b^+CD86^+Ly6C^{high}$), non-inflammatory myeloid cells ($CD11b^+Ly6C^{low}$) and DCs ($CD11b^+CD11c^+$), plotted data is expressed as min to max. Either treatments alone or combinational therapy induced the formation of pro-inflammatory dLNs state, but combinational therapy triggered the most significant changes, including infiltration of dLNs by neutrophils, increased levels of mature inflammatory myeloid cells and decreased proportions of non-inflammatory myeloid cells. (**K**) Flow cytometry analysis of DCs in dLNs and the violin graphs show the mean gMFI of CD86 and CD40 on DCs ($CD11b^+CD11c^+$) to indicate their activation. All treatment groups induced the infiltration and activation of DCs in the dLNs, and the most significant changes were observed in dLNs from combinational therapy-treated mice. (**L**) Flow cytometry analysis of lymphocyte influx into the TME after receiving different treatments of tumors. Plotted data is expressed as min to max. Living ($DAPI^-$) $CD45^+$ cells were further gated to $CD3^+$ T cells, $CD4^+$ T cells ($CD3^+CD4^+$), and $CD8^+$ T cells ($CD3^+CD8^+$). (**M**) Statistical evaluation of the percentage of circulating $CD3^+$, $CD4^+$ and $CD8^+$ T cells. Data are expressed as mean ± SEM (*$P < 0.05$, ** $P < 0.01$, *** $P < 0.001$, **** $P < 0.0001$). The combinational therapy treatment significantly increased the levels of $CD3^+$ and $CD4^+$ T cells in the blood compared to PDT, and the increase in $CD8^+$ T cells in the combinational therapy group was significantly different compared to the groups that received either monotherapy. (**N**) Total serum IgG concentrations of MC38 tumor-bearing mice in different subgroups on day 23 were assessed by ELISA. Data are expressed as mean ± SEM. The intensity of IgG in the serum of combinational therapy-treated mice was significantly improved compared to that of mice receiving PDT alone but not to the ADU-S100-treated group. (**O**) The dot graphs show functional immune memory T cells in the dLNs of cured mice by initial treatments at 21 days after tumor rechallenge. Living ($DAPI^-$) single cells were gated into $CD4^+$ central memory ($CD3^+CD4^+CD44^+CD62L^+$), the $CD4^+$ effector memory ($CD3^+CD4^+CD44^+CD62L^-$), $CD4^+$ naïve memory ($CD3^+CD4^+CD44^-CD62L^+$), $CD8^+$ central memory ($CD3^+CD8^+CD44^+CD62L^+$), the $CD8^+$ effector memory ($CD3^+CD8^+CD44^+CD62L^-$), and $CD8^+$ naïve memory ($CD3^+CD8^+CD44^-CD62L^+$). Age-matched naïve female mice ($n = 5$) were used as control and injected with the same amount of MC38 tumor cells. Detailed methods and materials are described in supplementary files. (**P**) Schematic illustration of our current working model by which PDT in combination with a STING agonist (ADU-S100) elicits anti-tumor immunity in colorectal cancer. 1). NIR irradiation allowed the photosensitizer to directly kill tumor cells via ROS but induced insufficient immune responses. 2). The combination of PDT and intratumoral ADU-S100 induced an inflammatory state in the TME and dLNs, thereby leading to a series of immune responses, including adaptive cellular and humoral immune responses. 3). ADU-S100 promotes the repolarization of M2 macrophages toward the M1 phenotype, relieving their immune inhibitory effects. The diagram was created at biorender.com. Abbreviations: three freeze/thaw cycle at -20°C (F/T); 4',6-diamidino-2-phenylindole (DAPI); analysis of variance (ANOVA); bone marrow-derived macrophages (BMDMs); cyclic GMP-AMP synthase (cGAS); colorectal cancer (CRC); dendritic cells (DCs); Enzyme-Linked ImmunoSorbent Assay (ELISA); geometric mean fluorescence intensity (gMFI); hematoxylin and eosin (H&E); immunoglobulin G (IgG); interferon (IFN); interleukin (IL); major histocompatibility complex (MHC); near-Infrared (NIR); photodynamic therapy (PDT); reactive oxygen species (ROS); Real-time quantitative reverse transcription PCR (qRT-PCR); standard error (SEM); stimulator of interferon genes (STING); T cell receptor (TCR); tumor microenvironment (TME); tumor-draining lymph nodes (dLNs); tumor necrosis factor (TNF); verteporfin (VP).

These cytokines play a key role during initial inflammation and the transition to T-cell-mediated immune responses.

Next, we analyzed the immune cell populations in the tumor, spleen and dLNs ten days after tumor inoculation. The results showed that either treatment alone or PDT and ADU-S100 combined induced the formation of a pro-inflammatory dLNs state, but the combinational therapy triggered the most significant changes, including infiltration of dLNs by neutrophils, increasing levels of mature inflammatory myeloid cells and decreasing proportions of non-inflammatory myeloid cells (Figure 1J). Rapid recruitment and an increase in neutrophil numbers are manifestations of acute inflammation and can initiate anti-tumor adaptive immune responses under inflammatory conditions [6]. Moreover, combinational therapy increased DC numbers and induced relatively enhanced DCs activation in dLNs compared with control or PDT alone (Figure 1K). The tumors treated with the combination exhibited significantly more infiltration of cytotoxic T lymphocytes (CTLs, $CD8^+$ T cells) than helper ($CD4^+$) T cells into the TME compared to tumors treated with monotherapies or control (Figure 1L). Of note, changes in the proportions of $CD4^+$ lymphocytes and CTLs in the spleen and dLNs were not significantly different (Supplementary Figure S6). These data proved that the combinational therapy amplified the effects of monotherapies on the immune-enhancing transformation of the TME and dLNs.

Local treatments have the potential to trigger systemic immune responses and, in some cases, the potential to exert an abscopal effect [7]. Hence, we examined the levels of circulating lymphocytes and total serum immunoglobulin G (IgG) in mice that received different treatments. On day 16, few changes and moderate increases in circulating $CD3^+$ and $CD4^+$ lymphocytes and CTLs were observed in PDT-treated mice and ADU-S100-treated mice. Importantly, the combination treatment significantly increased the levels of $CD3^+$ and $CD4^+$ T cells in the blood compared to PDT, and the increase in CTLs in the combined treatment group was higher compared to the monotherapy groups (Figure 1M and Supplementary Figure S7A-B). Of note, elevated expression of costimulatory CD40 on $CD19^+$ B cells, as well as increased IgG levels in blood serum, were observed on day 23 after combinational therapy (Figure 1N and Supplementary Figure S7C-D**)**. This was probably mediated by the activation of $CD4^+$ and $CD8^+$ cells. These activated cells produce interferon (IFN)-γ, which in turn can activate $CD19^+$ B cells to undergo isotype switching to produce more IgG. These data collectively suggest that the PDT and ADU-S100 combined treatment could establish systemic immune responses in vivo, including an enhanced proliferation of lymphocytes and antibody production in peripheral blood, which is essential for complete tumor eradication [8, 9].

Next, we examined the potential of established peripherally initiated systemic immunity to produce long-term immune memory and regulate distant tumors. Indeed, the mice that were cured by monotherapy and combined treatment all resisted tumor growth after rechallenging; this was in contrast to naïve controls that exhibited rapid tumor growth. Through immune memory phenotype analysis of the blood, dLNs and spleen of these mice, a trend of increased infiltration of functional memory $CD4^+$ and $CD8^+$ T cells was observed in ADU-S100 and combinational therapy treatment groups compared to control (Figure 1O and Supplementary Figure S8). Importantly, the mice cured by combinational therapy exhibited the most significant changes, especially in the dLNs (Figure 1N). This finding suggests that combined treatment resulted in the most prominent development of systemic memory immunity after tumor cell rechallenge following tumor eradication.

Moreover, both primary and distant tumor growth were inhibited or ablated by PDT, ADU-S100 or the combination treatment in the MC38 bilateral tumor model (Supplementary Figure S9). Although the combination treatment did not exert a higher tumor control effect on the distant untreated tumors than ADU-S100 treatment alone [10], it increased the survival rate of the mice bearing two MC38 tumors to 40% compared to that in the PDT (0%) and ADU-S100 (20%) groups (Supplementary Figure S9C). A similar effect of delaying untreated tumor growth was also observed in the CT26 bilateral model (Supplementary Figure S10). Together with previous results, the rationale underlying our current working model is shown in Figure 1P.

In conclusion, we provided first-hand evidence that combinational PDT and STING agonist treatment has an amplified inhibitory regulation on tumor growth and recurrence by the induction of anti-tumor immunity in established CRC models. Further studies are needed to identify the function of important factors in the TME, such as other immune cells and endothelial cells, during treatment.

DECLARATIONS

AUTHOR CONTRIBUTIONS

Original data collection and analysis, or interpretation - Yang Hao, Zili Gu, Sen Ma; writing - original draft preparation - Yang Hao; writing - review and editing - Zili Gu, Timo Schomann, Yuanyuan He, Xiaoxu Dong, Alireza Haghparast; figure - Yang Hao, Zhenfeng Yu; supervision - Peter ten Dijke and Luis J Cruz; Final additions - Peter ten Dijke and Luis J Cruz. All authors contributed to the article and approved the submitted version.

ACKNOWLEDGMENTS

We are grateful to Ferry Ossendorp (Department of Immunology, Leiden University Medical Center) for valuable discussion, Marcel Camps (Department of Immunology, Leiden University Medical Center) and the Ear-Nose-Throat (ENT) department for technical assistance and appreciate the support of all group members.

COMPETING INTERESTS

The authors declare that they have no competing interests. The authors declare that they have no conflict of interest.

FUNDING

Yang Hao received finacial support from the China Scholarship and Jilin Province Chinese Postdoctoral International Exchange Program (YJ20220406). Zili Gu, Zhenfeng Yu and Sen Ma received financial support from the China Scholarship Council, and Peter ten Dijke received funding from Cancer Genomics Centre Netherlands. Timo Schomann and Alireza Haghparast received funding from the European Commission, grants H2020-MSCA-RISE CANCER (777682) and H2020-WIDESPREAD-05-2017-Twinning SIMICA (852985).

AVAILABILITY OF DATA AND MATERIALS

The data presented in this study are available on request from the corresponding authors.

ETHICS APPROVAL AND CONSENT TO PARTICIPATE

This study was performed in line with the principles of the Dutch Animal Ethical Commission with the license of project AVD116008045 and approved by the Animal Experimental Committee from the Leiden University Medical Center (LUMC).

CONSENT FOR PUBLICATION

Not applicable.

Yang Hao[1,2]
Sen Ma[3]
Zili Gu[1]
Alireza Haghparast[4,5]
Timo Schomann[1,4]
Zhenfeng Yu[1]
Yuanyuan He[1]
Xiaoxv Dong[6]
Luis J Cruz[1]
Peter ten Dijke[7]

[1]*Translational Nanobiomaterials and Imaging (TNI) Group, Department of Radiology, Leiden University Medical Center, ZA Leiden, the Netherlands*
[2]*Department of Laboratory Animals, College of Animal Sciences, Jilin University, Changchun, China*
[3]*Department of Ophthalmology, Leiden University Medical Center (LUMC), ZA Leiden, the Netherlands*
[4]*Percuros B.V., CL Leiden, the Netherlands*
[5]*Immunology Section, Department of Pathobiology, Faculty of Veterinary Medicine, Ferdowsi University of Mashhad., Mashhad, Iran*
[6]*School of Chinese Material Medica, Beijing University of Chinese Medicine, Beijing, P. R. China*
[7]*Department of Cell and Chemical Biology and Oncode Institute, Leiden University Medical Center, RC Leiden, the Netherlands*

Correspondence
Luis J Cruz, Translational Nanobiomaterials and Imaging (TNI) Group, Department of Radiology, Leiden University Medical Center, ZA Leiden, the Netherlands
Email: L.J.Cruz_Ricondo@lumc.nl

Peter ten Dijke, Department of Cell and Chemical Biology and Oncode Institute, Leiden University Medical Center, RC Leiden, the Netherlands
Email: p.ten_dijke@lumc.nl

ORCID

Yang Hao https://orcid.org/0000-0003-2708-530X
Alireza Haghparast https://orcid.org/0000-0002-1905-6157
Timo Schomann https://orcid.org/0000-0002-0948-6209
Yuanyuan He https://orcid.org/0000-0003-0156-5671
Peter ten Dijke https://orcid.org/0000-0002-7234-342X

REFERENCES

1. Allison RR, Moghissi K. Photodynamic Therapy (PDT): PDT Mechanisms. Clin Endosc. 2013 Jan;46(1):24-9.
2. Castano AP, Mroz P, Hamblin MR. Photodynamic therapy and anti-tumour immunity. Nat Rev Cancer. 2006 Jul;6(7):535-45.
3. Turubanova VD, Balalaeva IV, Mishchenko TA, Catanzaro E, Alzeibak R, Peskova NN, et al. Immunogenic cell death induced by a new photodynamic therapy based on photosens and photodithazine. J Immunother Cancer. 2019 Dec 16;7(1):350.
4. Cheng N, Watkins-Schulz R, Junkins RD, David CN, Johnson BM, Montgomery SA, et al. A nanoparticle-incorporated STING activator enhances anti-tumor immunity in PD-L1-insensitive models of triple-negative breast cancer. JCI Insight. 2018 Nov 15;3(22):e120638.

5. Deng L, Liang H, Xu M, Yang X, Burnette B, Arina A, et al. STING-Dependent Cytosolic DNA Sensing Promotes Radiation-Induced Type I Interferon-Dependent Anti-tumor Immunity in Immunogenic Tumors. Immunity. 2014 Nov 20;41(5):843-52.
6. Leliefeld PH, Koenderman L, Pillay J. How Neutrophils Shape Adaptive Immune Responses. Front Immunol. 2015 Sep 14;6:471.
7. Spitzer MH, Carmi Y, Reticker-Flynn NE, Kwek SS, Madhireddy D, Martins MM, et al. Systemic Immunity Is Required for Effective Cancer Immunotherapy. Cell. 2017 Jan 26;168(3):487-502.e15.
8. Kleinovink JW, Fransen MF, Löwik CW, Ossendorp F. Photodynamic-Immune Checkpoint Therapy Eradicates Local and Distant Tumors by CD8+ T Cells. Cancer Immunol Res. 2017 Oct;5(10):832-8.
9. Corrales L, Glickman LH, McWhirter SM, Kanne DB, Sivick KE, Katibah GE, et al. Direct Activation of STING in the Tumor Microenvironment Leads to Potent and Systemic Tumor Regression and Immunity. Cell Rep. 2015 May 19;11(7):1018-30.
10. Alvarez M, Molina C, De Andrea CE, Fernandez-Sendin M, Villalba M, Gonzalez-Gomariz J, et al. Intratumoral co-injection of the poly I:C-derivative BO-112 and a STING agonist synergize to achieve local and distant anti-tumor efficacy. J Immunother Cancer. 2021 Nov;9(11):e002953.

SUPPORTING INFORMATION

Additional supporting information can be found online in the Supporting Information section at the end of this article.